The effect of the extent of polymerisation of a slag structure on the strength of alkali-activated slag binders

Keeley, P. M.; Rowson, N. A.; Johnson, T. P.; Deegan, D. E.

DOI:
10.1016/j.minpro.2017.05.007

Document Version
Peer reviewed version

Citation for published version (Harvard):
Keeley, PM, Rowson, NA, Johnson, TP & Deegan, DE 2017, 'The effect of the extent of polymerisation of a slag structure on the strength of alkali-activated slag binders', *International Journal of Mineral Processing*, vol. 164, pp. 37-44. https://doi.org/10.1016/j.minpro.2017.05.007

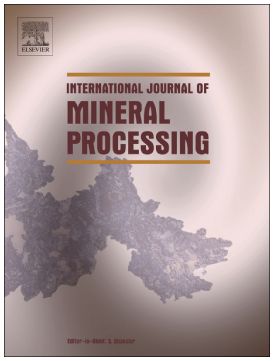

The effect of the extent of polymerisation of a slag structure on the strength of alkali-activated slag binders

P.M. Keeley, N.A. Rowson, T.P. Johnson, D.E. Deegan

PII: S0301-7516(17)30109-6
DOI: doi: 10.1016/j.minpro.2017.05.007
Reference: MINPRO 3049

To appear in: *International Journal of Mineral Processing*

Received date: 5 December 2016
Revised date: 18 April 2017
Accepted date: 17 May 2017

Please cite this article as: P.M. Keeley, N.A. Rowson, T.P. Johnson, D.E. Deegan , The effect of the extent of polymerisation of a slag structure on the strength of alkali-activated slag binders, *International Journal of Mineral Processing* (2017), doi: 10.1016/j.minpro.2017.05.007

The Effect of the Extent of Polymerisation of a Slag Structure on the Strength of Alkali-Activated Slag Binders.

P.M. Keeley[1,2], N.A. Rowson[1], T.P. Johnson[2], D.E. Deegan[2]

[1] School of Chemical Engineering University of Birmingham, Edgbaston, Birmingham, United Kingdom, B15 2TT.

[2]Tetronics International Marston Gate, South Marston Park, Swindon, Wiltshire, United Kingdom, SN3 4DE.

Keywords

Slag composition; slag basicity; plasma vitrification; alkali activation of slag; slag valorisation.

Abstract

Slags produced as industrial by-products can be used to replace cement by producing alkali-activated slag (AAS) binders. Slags are produced from a variety of high temperature processes and the composition of the slag will change depending on its origin. This paper presents work which investigated the effect of the chemical composition of the slag on its silicate glass network structure and how this affects the performance of the slag during alkali-activation. Several different slag compositions were obtained and Raman spectroscopy was used to determine the silicate structure present in the slags. Mechanical strength testing and dissolution experiments were used to assess the performance of the slags during alkali-activation. The results show that the chemical composition effects the polymerisation of the slag and a decrease in polymerisation of the slag's network structure leads to an increase in the strength of the AAS binder and greater slag reactivity.

Introduction

The reaction between a slag and an alkaline solution produces a paste which can develop a high compressive strength and is an alternative to traditional cement based binders used in the production of concretes. The product of this reaction is usually a calcium-silicon-aluminium-hydrate (C-A-S-H) or calcium-sodium-silicon-aluminium-hydrate (C-(N)-A-S-H) gel analogous to calcium silicate hydrate (C-S-H) which is the product of cement hydration[1]. This (C-A-S-H) gel can harden and develop the high compressive strengths required for construction materials[2].

These alkali-activated slag (AAS) pastes have been of interest since the 1950s[3], but they have not yet found extensive commercial use. However, finding applications for industrial by-products which gives them an intrinsic economic value is becoming increasingly important. This would enhance process economics and divert material from landfill, therefore avoiding gate fee costs. There is also an environmental benefit to replacing cement with an industrial by-product, since it has been reported that cement production accounts for between 5 to 8% of the world's CO_2 emissions[4]. Such a move would reduce the carbon impact of construction projects significantly.

Research on alkali-activated slags has, for the most part, focused on ground granulated blast furnace slags (GGBFS)[5][6] produced during iron making. However, GGBFS has a fairly narrow composition range and there are various high temperature processes producing slags of wider compositions which may also be suitable for producing AAS pastes[7]. For example slags of various compositions are produced from the treatment of wastes using DC plasma arc furnaces.

Thermal plasma technology is commonly used for the recovery of platinum group metals (PGMs), gold, silver and other economically valuable metals from end of life materials such as spent catalysts and electronic waste [8] and for the vitrification of hazardous materials such as air pollution control residue (APCr) or bottom ashes from municipal waste incineration plants[9][10]. The plasma process produces a vitreous, non-hazardous slag and when it is finely ground, displays pozzolanic activity and the ability for it to undergo alkali-activation[11][12]. A typical precious metal recovery plant would produce around 3,000 to 4,000 tonnes per year of slag and a vitrification plant treating air pollution control residue could produce between 30,000 to 50,000 tonnes per year of slag. Such a volume of material would be of interest to the concrete industry. The slags produced from the plasma processes are of various compositions depending on the material which is treated. It is therefore desirable to understand how these changes in composition effects the performance of a slag under alkali activation.

There have been numerous studies which have focused on the effect of compositional variations on the properties of alkali-activated binders and in particular, geopolymers and this work has mostly focused on the characteristics of the gel phase. However, this work focuses its attention on the effect of composition on the dissolution of the precursor during the first stage of the C-A-S-H gel formation mechanism of which there has been fewer studies. The work also focuses on slags which are not ground granulated blast furnace slags and so attempts to understand the effect of a wider range of compositions on the ability of slags to undergo alkali-activation.

The properties of the binding gel phase have been shown to be effected by the Si/Al ratio, the alkali cation content and the calcium content. Most of the work has focused on metakaolin and fly ash based geopolymers, but the properties of the gel phase produced from the alkali-activation of slag is similar. An increasing Si/Al ratio in the paste leads to geopolymers with greater mechanical strengths, but also increased stability in the geopolymer structure which reduces to tendency of the system to form zeolite crystalline structures which is observed at low Si/Al ratios[13,14]. The presence of aluminium is important due to its role in promoting the hardening of the gel phase[15]. Alkali metals present in the activating solution firstly facilitate the liberation of silicon and aluminium species from the precursor and then to alleviate the charge imbalance caused by the substitution of Al^{3+} for Si^{4+} in the geopolymer framework[16]. This leads to the formation of a N-A-S-H gel which is characteristic of geopolymers. When small amount of calcium ions are present in the system, there is little affect as they substitute in for the Na^{+} or K^{+} ions as charge balancers[17]. However, when the calcium concentration increases further, the formation of a C-A-S-H gel is preferred and a breakdown in the three-dimensional network structure of geopolymers occurs and the co-formation of C-S-H phases alongside the C-A-S-H phase which has been observed in high calcium containing fly ash and slag based geopolymers[18, 19] which can increase the compressive strength of the material. This breakdown in the three-dimensional framework and the move away from a N-A-S-H gel to a C-A-S-H demonstrates the difference between a geopolymer and an alkali-activated slag binder.

In the production of alkali-activated slag pastes, first stage of the reaction mechanism is the dissolution of the slag into the alkaline solution, releasing the Si and Al species required for the gel phase formation[13]. Therefore, the strength of the AAS binders is dependent on the solubility of the slag in an alkaline solution. This solubility can be affected by the particle size of the glass, the glass volume fraction of the slag and also its composition and structure[15,20].

The structure of vitreous slag can be described as a randomly orientated silicate network consisting of silicate tetrahedra (SiO_4)[21]. Each silicon atom is surrounded by four oxygens and each oxygen is bonded to two silicon atoms forming a random 'chain-like' network. As other components are added to the glass this network structure is altered depending on whether the new component is a 'network former' or a 'network modifier'.

Network modifiers disrupt the -Si-O-Si- bond causing some of the oxygen atoms to become non-bridging oxygens (NBO) i.e. no longer bridging silicon tetrahedra. As the amount of network modifiers increases, the number of non-bridging oxygens increases, or the (NBO/Si) ratio increases, causing the polymerisation of the silicate network to decrease[22][23]. Network formers on the other hand increase the polymerisation of the silicate network as they preferably co-ordinate with network modifiers and so increases or stabilises -O-Si-O- bonds in the network[24]. Table 1 gives an overview of the common network formers and modifiers (basic oxides) present in the slags studied. Al_2O_3 and Fe_2O_3 are amphoteric oxides which can act as either acidic or basic oxides present in a slag, although in the case of iron Fe^{2+} is thought of as a network modifier.

Table 1: Common network formers and modifiers in silicate glasses

Network Modifiers (Basic oxides)	Network Formers (Acidic oxides)	Amphoteric Oxides
Na_2O	SiO_2	Al_2O_3
CaO	TiO_2	Fe_2O_3
MgO	P_2O_5	
FeO		

The composition of a slag can be described by its 'basicity'. A slag's basicity increases as the concentration of network modifiers in its composition increases and a higher basicity indicates a greater degree of depolymerisation of the slag. There are several equations which have been used in the literature to describe a slag's basicity or depolymerisation. Most of these equations calculate the basicity of a slag by the molar ratio of basic oxides (network modifiers) over acidic oxides (network formers). In the field of geopolymers, researchers have used equation (1) to describe the 'depolymerisation' (DP) of ground granulated blast furnace slags[15,18]:

$$DP = \frac{n(CaO) - 2n(MgO) - n(Al_2O_3) - n(SO_3)}{n(SiO_2) - 2n(MgO) - 0.5n(Al_2O_3)} \quad (1)$$

Although a good correlation between a slag's reactivity during geopolymerisation and the calculated DP has been reported, this equation is specific to GGBFS and its narrow composition designed to control the production of iron. Therefore, it is not suitable to be used for slags derived from other processes, which may have high levels of TiO_2 for example, and it does not consider the effect of other oxides such as Fe_2O_3 or Na_2O.

The concept of optical basicity has also been used to describe the polymerisation of a slag's network structure. It has been used by researchers when attempting to develop models for predicting the viscosity, density and sulphide capacity of slag[25-27] as these properties rely, in part, on the polymerisation of the silicate network. The benefit of the concept of optical basicity is that it involves all components of the slag and so is more flexible to be used for a wider range of slag compositions.

The term 'optical' refers to the use of ultra-violet (UV) spectroscopy used to experimentally determine the basicity of the glass components.

The optical basicity of a multi-component slag can be calculated by equation (2):

$$\Lambda = \frac{\sum x_i n_i \Lambda_i}{\sum x_i n_i} \quad (2)$$

Where x_i is the molar fraction of component i, n is the number of oxygens in the component i.e. n = 2 for SiO_2, 3 for Al_2O_3 etc. and Λ_i is the optical basicity of component i.

The optical basicity for a component Λ_i can be calculated for using Pauling's electronegativity value χ_i for the metal in the component from the empirical equation (3):

$$\Lambda_i = \frac{1}{1.36(\chi_i - 0.26)} \quad (3)$$

The work presented in this paper investigates the effect of the polymerisation of a slag's structure on the strength of the alkali-activated binder which is produced when the slag undergoes alkali-activation. Raman spectroscopy and the optical basicity was used to determine the extent of polymerisation of the slag samples and compared the results to the slag's performance during alkali-activation via mechanical strength tests and dissolution experiments.

Methods and Materials

Slag from the vitrification of air pollution control residue was obtained from Tetronics International in Swindon, UK (the original sample reference is S1) and the composition altered to produce slag compositions similar to those produced via other plasma processes (PGM recovery processes for example) by adding TiO_2, CaO, SiO_2 and Al_2O_3 powders mixing with the slag then re-melted in a muffle furnace at 1600 °C to ensure the dissolution of the components into the slag before being air quenched to form a vitreous material. The slag was then ground using a planetary disc mill until the slag would pass through a 63 μm sieve.

The composition of the slags was determined using X-ray fluorescence (XRF) using a wavelength dispersive Bruker S8 Tiger XRF. X-ray diffraction (XRD) was performed on a Bruker D2 Phaser powder diffractometer to verify the vitreous nature of the slag prior to alkali-activation.

Small alkali-activated slag paste cylinders were made of a diameter of 13 mm and a height of 13 mm due to the small mass of each sample available. The compression strength testing was performed using a Zwick Z030 universal testing machine with a 50 kN load and a loading rate of 2 N/s. A total of six cylinders per slag were tested for their compressive strength. The alkali-activated cylinders were prepared by mixing 3 g of slag with 6 M NaOH with a solid/liquid ratio of 5 to form a workable paste. The mixture was placed in a die mould and compacted used a ram with a force of 40 MPa to produce cylinders. The cylinders were then kept in a controlled environment with 100 % humidity at 40 °C for 28 days for curing before testing.

Raman spectroscopy was performed on the ground slag samples using a Renishaw inVia Raman microscope with a 532 nm edge laser with a 50 cm filter. The peaks obtained using the Raman

microscope were deconvoluted using a peak fitting software (Fityk)[28] to determine the contributions of different silicate units.

Selective dissolution tests were performed on the alkali-activated slag binders following the method outlined by Luke and Glasser[29]. A solution of 1:1 ratio 0.05 M ethylene diamine tetraacetic acid in 0.1 M Na_2CO_3 was prepared and 9.5 ml was added to 0.95 ml of 1:1 triethanolamine:H_2O solution which was then mixed with 9.5 ml of distilled water. 25 mg of alkali-activated slag binders was added to this solution in a vial which was then put into an ultrasonic bath for 30 mins to aid dissolution. The solution was then vacuum filtered and the solid residue washed with distilled water and acetone before being dried to a constant weight and the mass weighed. The undissolved residue was then related to the initial mass used in the experiment to determine the % slag reacted.

Results

X-ray fluorescence (XRF) analysis

The compositions of the slag determined by XRF are shown in Table 2. In samples S1 to S3 the TiO_2 content is increased from 1.2 wt % to 16.6 wt %. The samples S4 to S8 have varied SiO_2, Al_2O_3, CaO and Na_2O content.

The optical basicity of the slags was calculated and ranged between 0.614 (S3) to 0.652 (S5). A higher optical basicity indicates a slag composition with a greater amount of basic oxides or network modifiers. In samples S1 to S3, the TiO_2 content in the slag increases and the optical basicity decreases corresponding to titanium dioxide's role as a network former. Sample S5 showed the highest optical basicity due to the relatively high levels of the network modifiers Na_2O and CaO.

Table 2: XRF analysis of the slag samples showing mass % of oxide components.

Oxide (wt %)	**S1**	**S2**	**S3**	**S4**	**S5**	**S6**	**S7**	**S8**
SiO_2	43.7	43.8	38.6	32.7	34.3	37.3	40.3	42.9
Al_2O_3	9.8	10.6	9.1	27.8	17.7	19.5	16.3	9.9
CaO	41.7	38.0	33.5	32.8	37.1	28.4	35.6	42.2
TiO_2	1.2	5.4	16.6	1.2	1.1	1.3	1.4	1.9
Na_2O	0.2	0.3	0.2	1.2	5.2	8.1	0.7	0.5
MgO	1.5	1.3	1.1	1.4	1.4	1.5	2.1	1.6
Fe_2O_3	1.2	0.3	0.4	2.0	2.6	2.8	2.3	0.4
P_2O_5	0.5	0.1	0.1	0.7	0.4	0.8	0.9	0.0
Total	99.8	99.8	99.6	99.8	99.8	99.7	99.7	99.4
Optical Basicity	0.630	0.620	0.614	0.629	0.652	0.629	0.620	0.634

X-ray diffraction (XRD) analysis

Figure 1 shows the XRD patterns of the slags used in the experiments. The patterns show a broad displacement between 35° and 45° 2θ which is characteristic of a vitreous slag showing no evidence of any crystalline phases in the slag and so suggests that the slags are at least 95 % amorphous. Crystalline phases are known reduce the effectiveness of the slag under alkali-activation[30] due to the stability of these crystalline structures and their inability to dissolve in alkaline solutions.

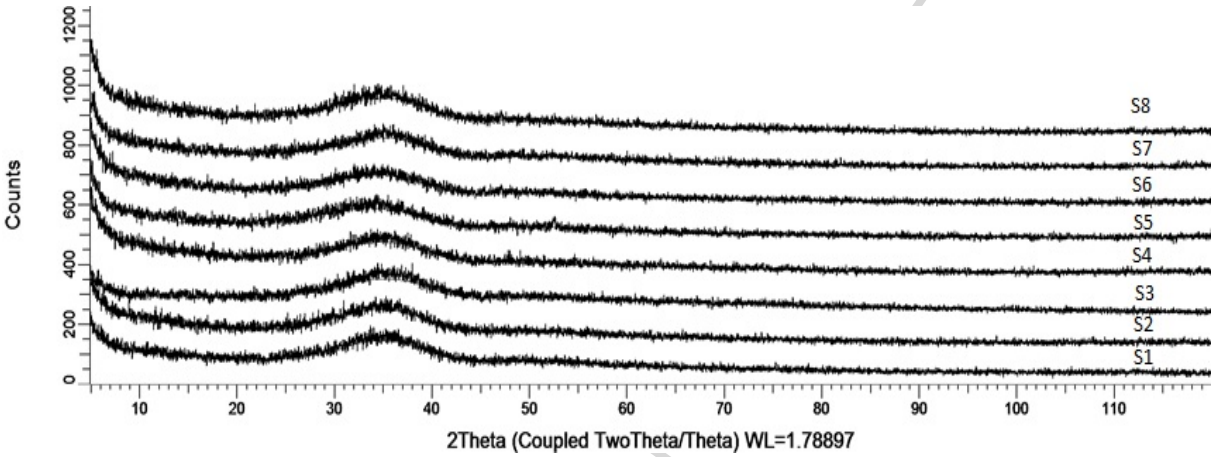

Figure 1: XRD patterns of slag samples showing a characteristic amorphous displacement between 35° and 45° 2θ.

Raman Spectroscopy

Raman spectroscopy is a useful technique to analyse the structure of silicate glasses and slags and has been used by numerous researchers to determine the changes in the glass structure due to the additions of components to the glass[31-33]. Table 3 shows the Raman frequencies of the stretch vibrations of anionic structural species in silicate melts.

Table 3: Raman frequencies of silicate structural species[31].

Q^n_{Si}	Structural Unit	NBO/Si	Frequency (cm^{-1})
Q^0_{Si}	SiO_4^{4-}	4	850-880
Q^1_{Si}	$Si_2O_7^{6-}$	3	900-920
Q^2_{Si}	$Si_2O_7^{4-}$	2	950-980
Q^3_{Si}	$Si_2O_5^{2-}$	1	1050-1100
Q^4_{Si}	SiO_2	0	1060-1190

Due to the complexity of the slag's structure the Raman spectra which were obtained for the slags were broad and diffuse, partly due to the non-crystalline nature of the slag, but also due to the combination of the different species present which causes peak overlap[22]. Therefore, the spectrum had to be deconvoluted and peaks fitted using computer software to determine which peaks are present in the spectrum. An example of the deconvolution is shown in Figure 2.

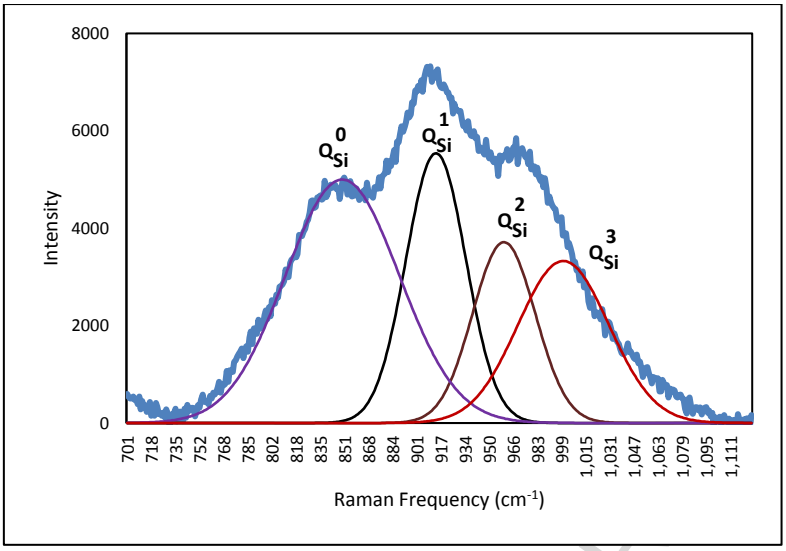

Figure 2: Deconvolution of Raman spectrum for S7

The Raman spectra for the slag samples 1, 2 and 3 which have a TiO_2 content of 1.2, 5.4 and 16.6 wt% respectively are shown in Figure 3 and the deconvoluted peak numbers can be seen in Table 4. As the TiO_2 content increases there is a shift to the left of the Raman peak where peaks were fitted at 920 cm^{-1} for S1 802 cm^{-1} for S2 and 714 cm^{-1} for S3. This shift to the left can be attributed to the presence of Ti-O-Ti bonds and Si-O-Si symmetric bonding which has been identified by different researchers[31][34]. The shift to the left is past the ≈ 850 cm^{-1} which is usually associated with Q_{Si}^0 species and therefore not associated with a deploymerised network, but a more polymerised network formed by Si-O-Si stretching and Ti-O-Ti bonds. This is consistent with titanium species being network formers in silicate glasses which would cause the formation of a more polymerised silicate structure in the slag. It is believed that the addition of TiO_2 to the glass causes the titanium to decrease the number of non-bridging oxygen associated with the silicon tetrahedral because the network modifiers which were co-ordinated with the non-bonding oxygens become preferably co-ordinated with titanate anions[35] causing the formation of -Si-O-Si- linkages.

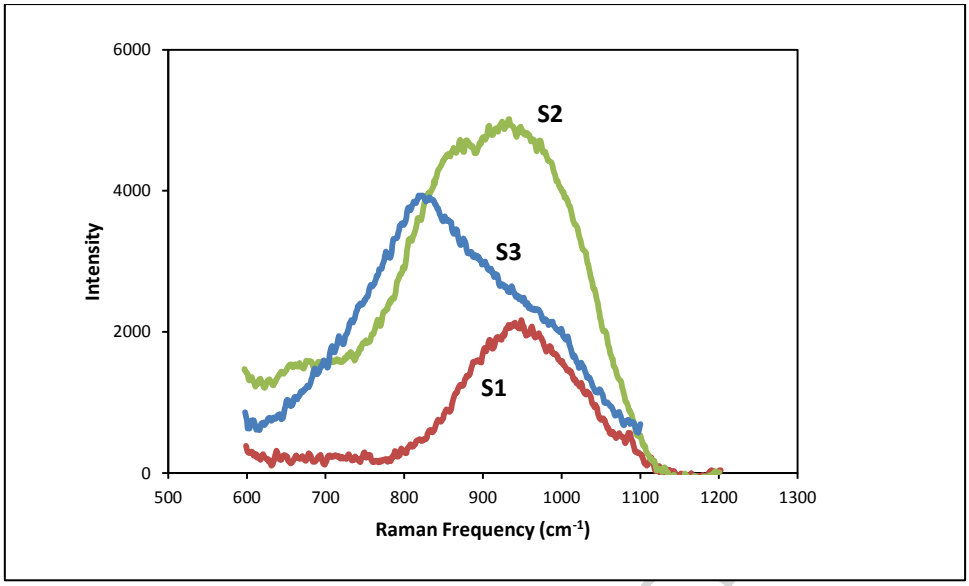

Figure 3: Raman spectra for S1, S2 and S3 which have an increasing TiO_2 content.

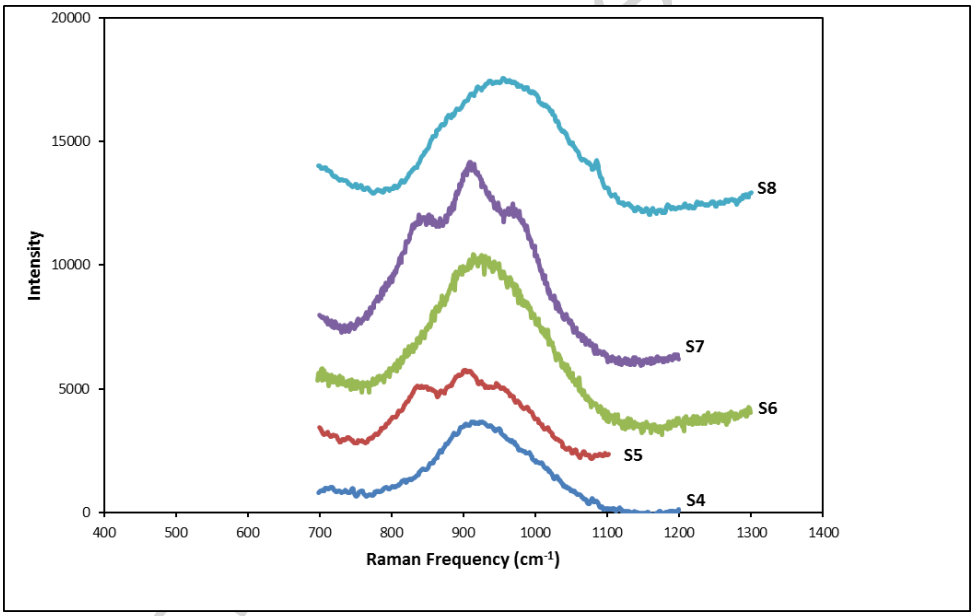

Figure 4: Raman spectra for slag S4 to S8 (offset data).

Figure 4 shows the Raman spectra for the slag samples 4 to 8. The data show different silicate species present in the slag samples and therefore different degrees of polymerisation in the glass. Slag samples S5 and S7 show the presence of Q^0_{Si} species in the glass due to shoulder peaks at 850 cm^{-1}. All the samples show some degree of depolymerisation with all peaks suggesting the presence of at least one non-bridging oxygen in the silicate structure.

The major components of all the slag samples are SiO_2, Al_2O_3 and CaO. The major structural component of the slag is the silicate network but the additions of aluminium and calcium oxygens can interfere with the network to reduce the polymerisation of the silicon tetrahedra. Aluminium can substitute with silicon tetrahedra in the network structure to form -Si-O-Al-O-Si bonds and so in this

way act as a network modifier. The introduction of aluminium into the network structure decreases the stability of the structure due to the Al-O bond being weaker than the Si-O bond which allows for a greater solubility in an alkaline solution. The calcium also acts as a network modifier by forming -Si-O-Ca bonds which, as these bonds increase, the tetrahedral network is reduced and so the depolymerisation of the silicate network increases[37, 38].

The optical basicity of the slag does, in general show a good correlation with the depolymerisation of the slag structure. The exception being sample S7 which shows the presence of Q^0_{Si} species despite having a low optical basicity. This indicates that the structure of the slag is dependant not wholly dependent on the composition, but also on other factors such as the thermal history (quench rate)[39].

Quantitative analysis of the volume fraction of the silicate species is not easy due to the different Raman scattering coefficients of the silicon tetrahedral species. Nevertheless, these results still show that there are clear differences in the slag structures due to confirmation of the presence of these species. A summary of Raman data for the slag samples is shown in Table 4.

Table 4: List of the deconvoluted peaks and structures found from Raman spectroscopy of the slag samples. The reference list indicates previous literature for peak assignment.

Sample	Deconvoluted peaks (cm^{-1})	Attribution	Reference
S1	920, 1000	Q^1_{Si} , Q^2_{Si}	[31]
S2	802, 907	Ti-O-Si or Ti-O-Ti, Q^1_{Si}	[31], [33]
S3	714, 819, 945	Si-O-Si symmetric bonding ,Ti-O-Si or Ti-O-Ti, Q^2_{Si}	[31], [33], [36]
S4	935	Q^2_{Si}	[31]
S5	850, 900, 960	$Q^0_{Si}, Q^1_{Si}, Q^2_{Si}$	[31]
S6	920, 939, 1000	$Q^1_{Si}, Q^2_{Si}, Q^3_{Si}$	[31]
S7	850, 914, 960, 1000	$Q^0_{Si}, Q^1_{Si}, Q^2_{Si}, Q^3_{Si}$	[31]
S8	920, 1000	Q^1_{Si}, Q^3_{Si}	[31]

Compression strength tests

The compression strengths, shown in Figure 5, varied between 97 MPa and 189 MPa. It must be noted that the high compression strengths are due to the small size of the cylinders and so are not representative of real world strengths of the material but are comparable to each other.

The addition on TiO_2 to the slag causes a decrease in the strength of the alkali-activated binders which is produced as the strength reduces from 138 MPa from sample S1 to 97 MPa with S3 which represents a 30% reduction in strength.

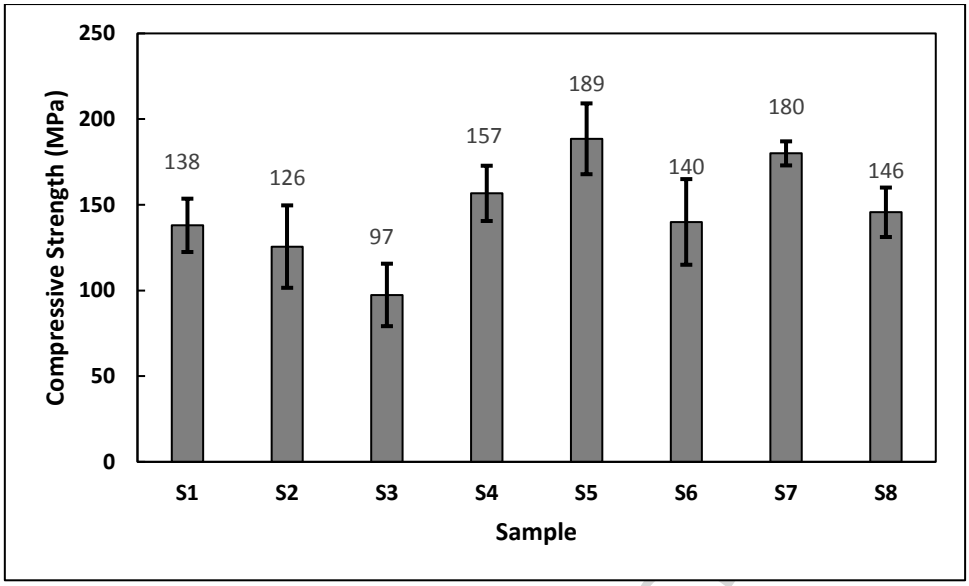

Figure 5: Compression strengths of the slag samples. Six samples per composition were tested. The error bars represent the standard deviation for each sample.

The highest strengths are achieved from samples S5 and S7 which show the presence of SiO_4^{4-} (Q_{Si}^0) which have four non-bridging oxygens indicating a high degree of depolymerisation in the slag structure. The samples which show a lower compression strength do not indicate the presence of the silicate species with 4 non-bridging oxygens and so have a higher degree of polymerisation and samples S6 and S8 which indicate the presence of Q_{Si}^3 have the lowest strength of samples S4 to S8. There is a 26% reduction in strength between the samples S5 and S6 as the slag structures become more polymerised. The results of the Raman spectroscopy indicate that the higher the degree of polymerisation in the slag structure, the lower the strength of the alkali-activated binder.

There is a good relation between the optical basicity and the compression strength of the slag samples shown in Figure 6. Despite S7 showing a strength which is not consistent with the general trend shown by the other samples, the data shows that the optical basicity is a good indicator of the reactivity of a slag.

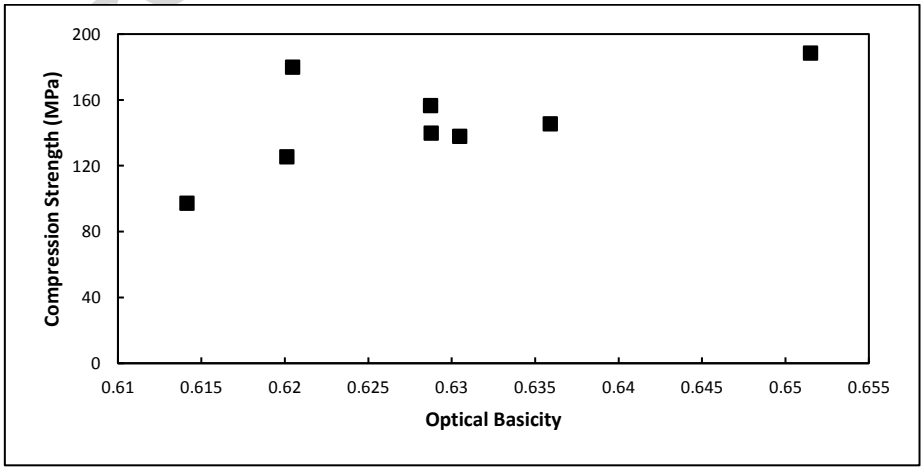

Figure 6: Compression strength of the slag samples vs the calculated optical basicity of the samples

Selective Dissolution

The concept of the selective dissolution test was to dissolve the gel phase reaction product and not the unreacted slag. There is a strong correlation between the % of reacted slag and the compression strength of the sample which was obtained which can be seen in Figure 7.

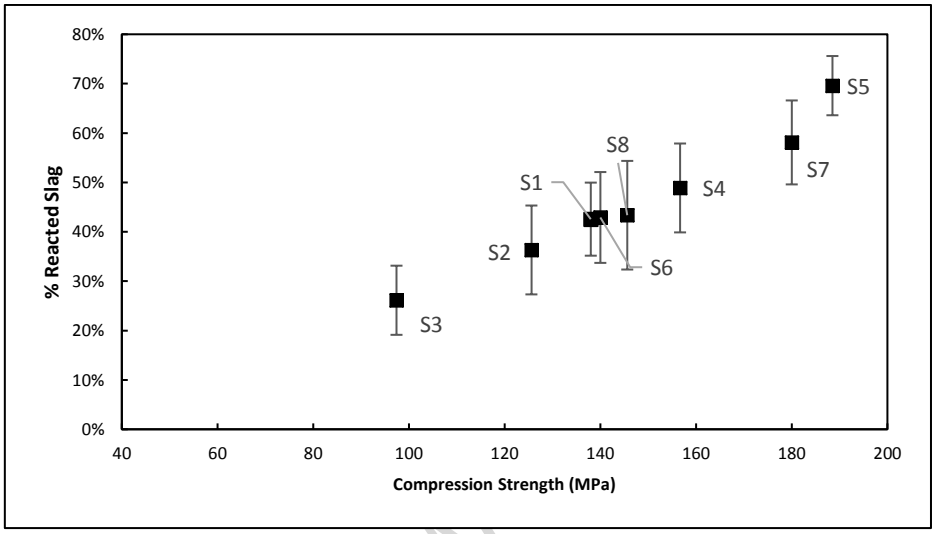

Figure 7: Selective dissolution of the alkali-activated slag binders showing the relationship between % slag reacted and the compression strength. The error bars indicate the standard deviation for each sample.

The results show that as more of the slag reacts, the greater the strength of the alkali-activated binder. The results range from 26 % to almost 70 % for the slags showing the highest compression strength. The higher the amount of dissolution of the slag would therefore lead to the higher amount of silicate and aluminate species dissolving into solution which then allows for the formation of the strength giving phase in the AAS binder. Although the reactivity of 22 % is low it is consistent with the reactivity of blast furnace slags when blended with cement acting as a pozzolan[40][41]. Scanning electron microscopy (SEM) images (Figure 8) of alkali-activated slag binder does show a high fraction of unreacted slag which is also consistent with the results obtained in this experiment.

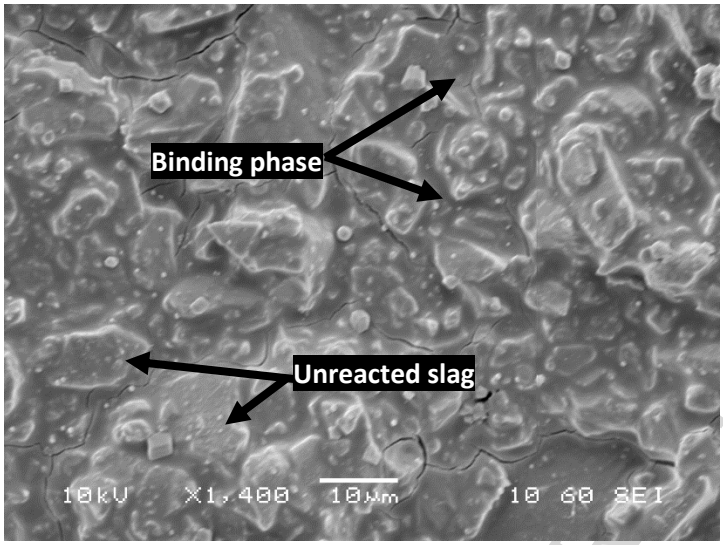

Figure 8: SEM image of alkali activated slag binder showing unreacted slag particles engulfed by the gel phase. (Image was taken from AAS binder from slag sample S1).

During the dissolution of the slag in the activating solution, the liberation of aluminium species is much greater than the liberation of silicon species. This is due to the Al-O bonds being more susceptible to breakage than Si-O bonds which are more stable. This is shown in Figure 9 which shows the rate of dissolution of aluminium to be much higher than that of silicon.

Therefore, it follows that the increasing amount of Si-O bonds in the slag would decrease the rate of dissolution of the species during alkali-activation, or the increasing polymerisation of the silicate network structure, which would result in a greater number of Si-O bonds would decrease the rate of dissolution.

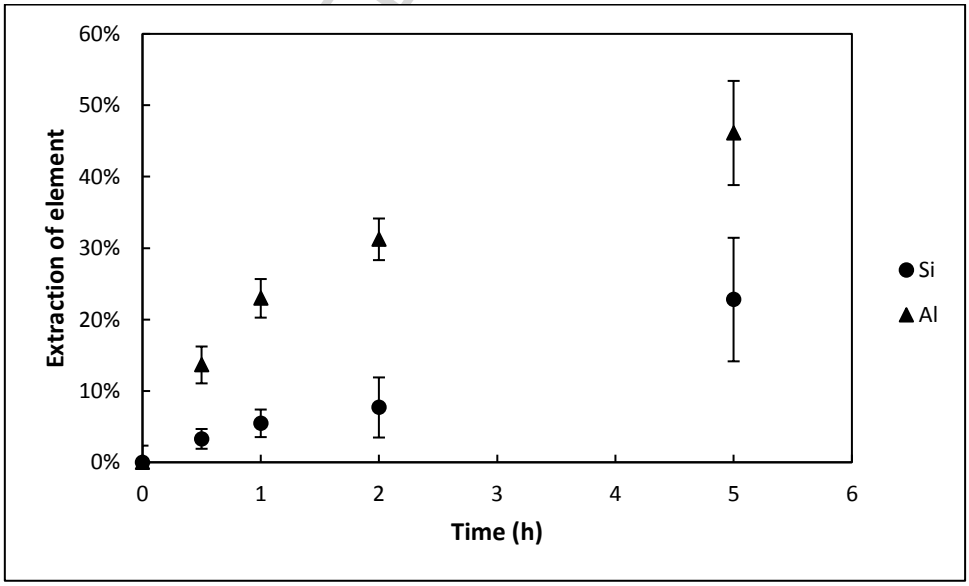

Figure 9: Dissolution of silicon and aluminium from slag (S1) over time in 10 M NaOH. Error bars indicate the standard deviation of the samples.

Discussion

The 'back bone' of the alkali-activated gel is an aluminosilicate network and so is dependent on the availability of silicon and aluminium species in solution to be able to form. The availability of these species is dependent on their dissolution from the slag during the first phase of the reaction mechanism. Therefore, the greater the solubility of the slag in an alkaline solution, the greater the strength of the gel phase formed.

The solubility of the slag in the alkaline solution is dependent on a number of characteristics and firstly it is important that the slag has a fine particle size and high glass volume fraction. In the cement industry, the glass fraction of GGBFS must be greater than 95 % for it to be used effectively as a pozzolan[42]. The results in this work has shown that the solubility of the slag is effected by its composition and the extent of the depolymerisation of the silicate network. The stability of -O-Si-O- bonds mean that the silicon species in the slag are not easily liberated. The incorporation of other components into the slag especially Ca^{2+} and Na^{+} ions disrupt the silicon oxygen linkages breaking down the silicate network. The incorporation of metal oxides in the slag causes the formation of -Si-$O^{-}(M^{+})$ complexes which as their concentration in the slag increases, reduce the number of bridging oxygens and so increase the reactivity of the slag. As the number of non-bridging oxygens increase, the liberation of Si and Al species from the slag increases at a high pH. The introduction of these components into the slag may be achieved via the addition of fluxing agents during the process which would enhance the performance of the slag during the alkali-activation. The composition of blast furnace slag and other types of smelting operations is optimised for metal production, but the slag chemistry for vitrification processes is more flexible and so their composition could be optimised for slag performance as a cement replacement – providing furnace operation is not compromised (refractory wear, energy costs etc.).

The composition of the slag and its depolymerisation are closely related, but they are not necessarily reliant on one another. This is shown by the good correlation between the compressive strength of the samples vs its optical basicity, but with a noticeable anomaly in sample S7. The depolymerisation of the silicate network can be caused by the presence of network modifiers such as CaO and Na_2O, but it is also dependent on the thermal history of the slag i.e. its quench rate. The samples used in this experiment were all quenched in the same way – in air, which was shown to be fast enough to ensure that a vitreous, X-ray amorphous structure was produced. However, an unexpected change in conditions may have caused a faster cooling rate in sample S7 to create greater depolymerisation in the structure causing a departure from the trend seen in the comparison between the compression strength and the optical basicity.

Nevertheless, the data obtain from the Raman spectroscopy indicates that a greater depolymerisation of the silicate structure does lead to a greater reactivity in of the slag and a higher compressive strength of the alkali-activated binder. This was shown in Figure 7 where the samples S2 and S3, which showed evidence of an increasingly depolymerised silicate network due to increasing levels of TiO_2, had the lowest reactivity and conversely, those samples which showed the evidence of the presence of Q^{0}_{Si} species had the greatest compression strengths and reactivity.

The properties of the binding phase being dependant on the Si/Al ratio means that the liberation of silicon from the slag is important to create pastes with high strengths or more stable gel structures.

As the full reaction of slag during alkali-activation cannot be assumed, a slag with a high SiO_2 content may not be as suitable for alkali-activation as one with a lower SiO_2 content because of the reduced reactivity of highly stabilised silicate structures in the slag. The use of an activating solution which contains available silicate species, such as sodium silicate solution, means that the slow release of silicon during the dissolution of the slag can be alleviated by the silicon species available in the activating solution. Therefore, any reduction of the strength which may be associated with the extent of the depolymerisation of the slag can be alleviated by the presence of the pre-dissolved silicon species. In this way, it would be possible to increase the Si/Al ratio required for a high strength and stable alkali-activated slag paste.

Conclusions

The strength of the alkali-activated slag is related to the extent of the dissolution of the slag in an alkaline solution. The higher the dissolution, the stronger the AAS binder. The slag's structure can be altered by the addition of network modifiers and network formers which can cause the decrease or the increase in the polymerisation of the silicate network respectively. The extent of the polymerisation of the silicate network in the slag influences the strength of the AAS binder by altering the solubility of the slag in an alkaline environment. Samples S5 and S7 showed the greatest strength due to the presence of depolymerised silicate units giving the slag better dissolution properties in the alkaline solution. The addition of titanium into the slag resulted in a decrease in strength of the alkali-activated slag binder which was due to an increase in the polymerisation of the silicate network which was seen by the Raman spectroscopy.

Acknowledgments

We would like to give our thanks to the Engineering and Physical Science Research Council (EPRSC) who funded with work and which was supported by Tetronics International Limited and the Centre for Formulation Engineering at the University of Birmingham. The EPRSC grant code is EP/G036713/1.

References

[1]Taylor, H. (1986), Proposed structure for calcium silicate hydrate gel. **Journal of the American Ceramic Society,** 69(6):464-67.

[2]Provis, J.L. Palomo, A. Shi, C. (2015), Advances in understanding alkali-activated materials. **Cement and Concrete Research**

[3]Pacheco-Torgal, F. Castro-Gomes, J, Jalali, S. (2008), Alkali-activated binders: A review: Part 1. Historical background, terminology, reaction mechanisms and hydration products. **Construction and Building Materials,** 22: 1305-1314.

[4]Deventer, J. Provis, J. Duxson, P. (2011), Technical and commercial progress in the adoption of geopolymer cement. **Minerals Engineering**, 29: 89-104.

[5]Haha, M. Lothenbach, B. Le Saout, G. Winnefeld, F. (2011), Influence of slag chemistry on the hydration of alkali-activated blast furnace slag – Part I: Effect of MgO. **Cement and Concrete Research,** 41:955-963.

[6]Burciaga-Diaz, O. Escalante-Garcia, J. (2013), Structure, mechanisms of reaction and strength of an alkali-activated blast furnace slag. **Journal of the American Ceramic Society,** 96: 3939-3948.

[7]Shi, C. Qian, J. (2000), High performance cementing materials from industrial slags – a review. **Resources, Conservation and Recycling** 29:195-207.

[8]Keeley, P.M. Rowson, N.A. Deegan, D.E. Stachowski, T. (2015), Platinum and rhenium recovery from reforming catalysts via plasma arc technology. **The Conference of Metallurgists**, Toronto Published by the Canadian Institute of Mining, Metallurgy and Petroleum, Montreal.

[9]Gomez, E. Amutha Rani, D. Cheeseman, C.R. Deegan, D. Wise, M. Boccaccini, A.R. (2008), Thermal plasma technology for the treatment of wastes: A critical review. **Journal of Hazardous Materials,** 161: 614-626.

[10]Amutha Rani, D. Boccaccini, D. Deegan, D. Cheeseman, C.R. (2008), Air pollution control residues from waste incineration: Current UK situation and assessment of alternative technologies. **Waste Management,** 28: 2279-92.

[11]Kourti, I. Amutha Rani, D. Boccaccini, R. Cheeseman, C.R. (2011), Geopolymers from DC plasma-treated air pollution control residues, metakaolin and granulated blast furnace slag. **Journal of Materials in Civil Engineering,** 23: 735-740.

[12]Kourti, I. Deegan, D. Boccaccini, R. Cheeseman, C.R. (2013), Use of DC plasma treated air pollution control (APC) residue glass as pozzolanic additive in Portland cement. **Waste Biomass Valorisation,** 4:719-728.

[13]Duxson, P. Fernandez-Jimenez, A. Provis, J.L. Lukey, G.C. Palomo, A. van Deventer, J.S.J. (2007), Geopolymer technology: the current state of the art. **Journal of Materials Science,** 42:2917-2933.

[14] He, P, Wang, M, Fu, S, et al. (2016), Effects of Si/Al ratio on the structure and properties of metakaolin based geopolymer. **Ceramics International.** 42:14416-14422.

[15]Duxson, P. Provis, J.L. (2008), Designing precursors for geopolymer cements. **Journal of the American Ceramic Society,** 12:3864-3869.

[16]Duxson, P. Provis, J.L. Lukey, G.C. Mallicoat, S.W. Kriven, W.M. van Deventer, J.S.L. (2005), Understanding the relationship between geopolymer composition, microstructure and mechanical properties. **Colloids and Surfaces A: Physicochemical Engineering,** 269:47-58.

[17] García-Lodeiro, I and Fernández-Jiménez, A (2010), Effect of calcium additions on N–A–S–H cementitious gels. **Journal of the American Ceramic Society.** 93(7):1935-1940.

[18] Li, C, Sun, H and Li, L (2010), A review: The comparison between alkali-activated slag (Si+ Ca) and metakaolin (Si+ Al) cements. **Cement and Concrete Research.** 40:1341-1349.

[19] Temuujin, J, Riessen, V.A. and Williams, R (2009), Influence of calcium compounds on the mechanical properties of fly Ash geopolymer Pastes. **Journal of Hazardous Materials.** 167:82-88.

[20]Fernandez-Jimenez, A. Palomo, J.G. Puertas, F. (1999), Alkali-activated slag mortars mechanical strength behaviour. **Cement and Concrete Research**, 29:1313-1321

[21]Brawer, S.A. and White, W.B. (1975), Raman spectroscopic investigation of the structure of silicate glasses. I. The binary alkali silicates. **The Journal of Chemical Physics,** 63(6):2421:2432.

[22]McMillan, P. (1984), Structural studies of silicate glasses and melts – applications and limitations of Raman spectroscopy. **American Mineralogist,** 69:622-644.

[23]Kalampounias, A.G. (2008), IR and Raman spectroscopic studies of sol-gel derived alkaline earth silicate glasses. **Bulletin of Material Science,** 34(2):299-303.

[24]Duffy, J.A. and Ingram, M.D. (1976), An interpretation of glass chemistry in terms of the optical basicity concept. **Journal of Non-Crystalline Solids,** 21:373-410.

[25] Hu, X, Ren, Z, Zhang, G, et al. (2012), A model for estimating the viscosity of blast furnace slags with optical basicity. **International Journal of Minerals,** 19(12):1088-1092.

[26] Zhang, G. and Chou, K. (2010), Model for Evaluating Density of Molten Slag With Optical Basicity. **Journal of Iron and Steel Research, International**, 17 (4): 1–4.

[27] Duffy, J.A., Ingram, M.D. and Sommerville, I.D. (1978), Acid-base properties of molten oxides and metallurgical slags. **Journal of the Chemical Society, Faraday Transactions 1: Physical Chemistry in Condensed Phases**, 74: 1410–1419.

[28]Wojdyr, M. (2010), Fityk: A general purpose peak fitting program. **Journal of Applied Crystallography,** 43:1126

[29]Luke, K. Glasser, F.P. (1987), Selective dissolution of hydrated blast furnace slag cements. **Cement and Concrete Research,** 17:273-282.

[30]Massazza, F. (1993), Pozzolanic cements. **Cement and Concrete research,** 15:185-214.

[31]Mysen, B. Virgo, D. Scarfe, C. (1980), Relations between anionic structure and viscosity of silicate melts – a Raman spectroscopic study. **American Mineralogist,** 65:690-710.

[32]McMillan, P. Wolf, G.H. Poe, B.T. (1991), Vibrational spectroscopy of silicate liquids and glasses. **Chemical Geology,** 96:351-366.

[33]Zheng, K. Junlin, L. Wang, X. Zhang, Z. (2013), Raman spectroscopy of CaO-MgO-SiO_2-TiO_2 slags. **Journal of Non-Crystalline solids,** 376:209-215.

[34]Neuville, D.R. Cormier, L. Massiot, D. (2006), Al coordination and speciation in calcium aluminosilicate glasses: Effect of composition determined by ^{27}Al MQ-MAS NMR and Raman spectroscopy. **Chemical Geology**, 229:173-185.

[35]Yadav, K.A. and Singh, P. (2015), A review of oxide glasses by Raman spectroscopy. **RSC Advances,** 5:67583-67609.

[36]Wang, M. Cheng, J. Li, M. He, F. (2011), Raman spectra of soda-lime-silicate glass doped with rare earth. **Physica B,** 406:365-3869.

[37] Biswas, A.K. and Bashforth, G.R. (1962), The Physical Chemistry of Metallurgical Processes. Chapter XIX – Slags pp 303-324. Chapman and Hall, London.

[38]Ryerson, F.J. and Hess, P.C. (1980), The role of P_2O_5 in silicate melts. **Geochimica et Cosmochimica,** 44:611-624.

[39]Tan. J. Zhao, S. Wang, W. Davies, G. Mo, X. (2003), The effect of cooling rate on the structure of sodium silicate glass. **Materials Science and Engineering B,** 106:295-299.

[40]Escalante, J.I. Gomez, L.Y. Johal, K.K. Mendoza, G. Mancha, H. Mendez, J. (2001), Reactivity of blast-furnace slag in Portland cement blends hydrated under different conditions. **Cement and Concrete Research,** 31:1403-1409.

[41]Dyson, H.M. Richardson, I.G. Brough, A.R. (2011), A combined ^{29}Si MAS NMR and selective dissolution technique for the quantitative evaluation of hydrated blast furnace slag cement blends. **Journal of the American Ceramic Society,** 90(2):598-602.

[42] British Standards Institute (2006), BS EN 15167-1, Ground granulated blast furnace slag for use in concrete, mortar and grout – Part 1: Definitions, specifications and conformity criteria. BSI Standards Limited 2006.

Paper highlights

- The polymerisation of a slag's structure affects its dissolution characteristics.
- The dissolution of the slag affects the strength of alkali-activated slag pastes.
- Increased polymerisation reduces the dissolution of the slag.
- The composition of the slag affects the polymerisation of its structure.